Published in final edited form as:
J Biomed Mater Res A. 2010 September 15; 94(4): 1100–1110. doi:10.1002/jbm.a.32781.

Fabrication of Cardiac Patch with Decellularized Porcine Myocardial Scaffold and Bone Marrow Mononuclear Cells

Bo Wang[1], **Ali Borazjani**[1], **Mina Tahai**[1], **Amy L. de Jongh Curry**[2], **Dan T. Simionescu**[3], **Jianjun Guan**[4], **Filip To**[1], **Steve H. Elder**[1], and **Jun Liao**[1]

[1]Cardiovascular Tissue Biomechanics Laboratory, Department of Agricultural and Biological Engineering; Computational Manufacturing and Design, CAVS, Mississippi State University, Mississippi State, MS

[2]Department of Biomedical Engineering, University of Memphis, Memphis, TN

[3]Department of Bioengineering, Clemson University, Clemson, SC

[4]Department of Material science and Engineering, Ohio State University, Columbus, OH

Abstract

Tissue engineered cardiac grafts are a promising therapeutic mode for ventricular wall reconstruction. Recently, it has been found that acellular tissue scaffolds provide natural ultrastructural, mechanical, and compositional cues for recellularization and tissue remodeling. We thus assess the potential of decellularized porcine myocardium as a scaffold for thick cardiac patch tissue engineering. Myocardial sections with 2 mm thickness were decellularized using 0.1% sodium dodecyl sulfate (SDS), and then reseeded with differentiated bone marrow mononuclear cells. We found that thorough decellularization could be achieved after 2.5 weeks treatment. Reseeded cells were found to infiltrate and proliferate in the tissue constructs. Immunohistological staining studies showed that the reseeded cells maintained cardiomyocyte-like phenotype and possible endothelialization was found in locations close to vasculature channels, indicating angiogenesis potential. Both biaxial and uniaxial mechanical testing showed a stiffer mechanical response of the acellular myocardial scaffolds; however, tissue extensibility and tensile modulus were found to recover in the constructs along with the culture time, as expected from increased cellular content. The cardiac patch that we envision for clinical application will benefit from the natural architecture of myocardial extracellular matrix, which has the potential to promote stem cell differentiation, cardiac regeneration, and angiogenesis.

1. INTRODUCTION

Each year, approximately one million Americans suffer myocardial infarction (MI) with a 10% in-hospital mortality rate.[1] If the amount of myocardium loss as a result of the MI is large, significant mechanical complications such as left ventricular dilatation, mitral regurgitation, and heart failure can occur.[2,3] Following cardiomyocyte death and scar formation in the infarcted region,[4] tissue remodeling, characterized by cardiac myocyte hypertrophy/apoptosis, fiber disarray, and increased collagen deposition may take place in regions remote from the infarcted region as a result of abnormal stress distribution.[5] Left ventricular remodeling may lead to pathological dilation and heart failure which in severe cases may progress to death. The main goal of MI treatment is to prevent the adverse

*Correspondence Author: Jun Liao, Ph.D., Assistant Professor, Department of Agricultural & Biological Engineering, Mississippi State University, 130 Creelman Street, Room 222, Mississippi State, MS 39762, Tel: 662-325-5987, Fax: 662-325-3853, jliao@abe.msstate.edu.

remodeling of the left ventricle that leads to heart failure.[6] Standard therapies include after-load reduction with angiotensin converting enzyme inhibitors and prompt, and as complete as possible, revascularization (both percutaneous and surgical) in order to limit the infarct size and prevent extension of the infarct. Despite standard therapies, some patients progress to a severe cardiomyopathy and are candidates for cardiac transplant, which is often limited by the availability of suitable donors.

Newer treatments such as cell therapies (myoblast/stem cell injection), intramyocardial gene transfer, and cardiac patch repair offer alternative therapeutic approaches.[7-9] Cardiac patch techniques have been developed to repair injured heart and restore cardiac function. Polymeric and tissue derived materials such as polytetrafluoroethylene (ePTFE), Dacron, and chemically treated pericardium have been used as patch material.[10,11] However, the limitations of nonviable patches include inflammatory response, mismatched mechanical properties, and thrombosis.[11] Recently, tissue engineering approaches have attracted interest. The basic concept of tissue engineering is to build a new tissue from cellular components using a scaffold to provide a structural guide.[12-15] In previous applications, tissue engineered patches were implanted over a region of infarcted cardiac tissue in order to stimulate angiogenesis in the damaged tissue and attenuate a reduction in cardiac function.[4,16-18]

The ideal engineered cardiac tissue provides optimal structural, mechanical, and electrophysiological properties maintained by viable transplanted cells, and might also stimulate the formation of vasculature supplying oxygen and nutrients in the patched region.[4,16] For this purpose, biodegradable scaffolds were often used as a template to support seeded cells. Collagen gel, alginate, porous pericardium, small intestinal submucosa, polyglycolic acid (PGA), poly (lactide-co-carolactone), and poly ester (urethane urea) have been used as supporting scaffold for cells.[4,10,19,20] Various cell types, such as bone marrow stem cells, umbilical stem cells, embryonic stem cells, fetal cardiomyocytes, smooth muscle cells, and dermal fibroblasts, were investigated as cell sources for patch recellularization.[21-25] Among them, bone marrow stem cells were found to have a capacity to regenerate myocardium, induce of angiogenesis, and be free from ethical issues.[7,17,19,20,25,26]

Myocardial tissue has complex muscle fiber architecture mediated by cardiac ECM networks and hence has unique cell to cell interconnections.[27-29] The question is how one can mimic this unique ECM network. Recently, tissue derived acellular scaffolds such as heart valves, skin, small intestinal submucosa, and urinary bladder have been investigated for tissue engineering/regeneration applications.[30-34] The advantages of decellularization approach are (i) efficient removal of all cellular and nuclear content and (ii) preservation of ECM composition, biologic activity, and mechanical integrity.[30] Moreover, major achievements in creating decellularized whole rat heart scaffolds have drawn considerable attention.[35] Ott et al.[35] reported that they successfully produced acellular, perfusable vascular architecture, competent acellular valves and intact chamber geometry using a rat heart. The acellular intact rat heart was then reseeded with cardiac and endothelial cells by a perfusion bioreactor. By day 8, under physiological load and electrical stimulation, macroscopic contractions were observed with a pump function equivalent to about 2% of adult or 25% of 16-week fetal heart function.[35] The next possible ambitious attempt is to apply this approach to larger xenogenous hearts, such as pig hearts that have similar size, anatomic geometry and vasculature systems as human. Many questions and technical hurdles, such as reseeding of thick tissue scaffold, feasibility of using existing vasculature network, and angiogenesis in thick tissues, need to be addressed before any scaled-up attempt.

The above successful applications imply the advantage of harnessing the optimal design by nature. We therefore investigated decellularized porcine myocardial scaffold as a potential template for cardiac patch tissue engineering. We hypothesize that decellularized porcine myocardium scaffold preserves natural ultrastructural, mechanical, and compositional cues for cardiac tissue regeneration and would provide optimal microenvironments for stem cell reseeding, cardiomyocyte differentiation, and angiogenesis. The objectives of this study were to create a cardiac patch using decellularized pig myocardium scaffold and bone marrow mononuclear cells (BMMCs), and assess its potential for tissue remodeling.

2. MATERIALS AND METHODS

2.1 Preparation of Acellular Porcine Myocardial Scaffold

Fresh porcine hearts were obtained from a local slaughter house and transported to the laboratory in PBS at 4 °C. Myocardial sections (15 × 15 × 2 mm) were dissected from the ventricular wall. The myocardium was decellularized in a rotating bioreactor using 0.1% sodium dodecyl sulfate (SDS) with 0.01% trypsin, 1 *m*M phenylmethylsulfonylfluoride (PMSF, protease inhibitor), 20□μg/ml RNase A and 0.2 mg/ml DNase for 2.5 weeks, Ten-minute ultrasonic treatment (50 HZ, Branson, US) was applied each day and the SDS solution was changed every two days.

2.2 Isolation of Porcine Bone Marrow Mononuclear Cells

Bone marrow was extracted from femurs and tibias of fetal pigs. Both ends of each femur or tibia were cut and the bone marrow was washed out with phosphate-buffered saline (PBS). Cells were centrifuged at 400 r/min for 10 min at 4°C, suspended by gentle pipetting, and cultured in mesenchymal stem cell (MSC) medium (Low-glucose Dulbecco's modified Eagle's medium (L-DMEM) with 5% fetal bovine serum (FBS), Mesenchymal Stem Cell Growth Supplement (Sciencell), and 100 U/ml penicillin and 100 μg/ml streptomycin (Invitrogen) at 37°C in a humid 5% CO_2 air atmosphere. Three days later, nonadherent cells were removed by replacing the medium. After 10 days' culture, the adherent cells were resuspended after HyQTase (Fisher safety) treatment and re-plated at a density of 2×10^4/cm^2. The medium was changed every 3 days. Bone marrow mesenchymal stem cell population was verified by stem cell CD44 surface marker staining (Abcam).

2.3 Myogenic Differentiation and Reseeding

The second passage BMMCs were re-suspended after 0.25% trypsin treatment and washed twice with Tyrode's balanced salt solution (Sigma). The cells were re-suspended in mesenchymal stem cell medium and seeded into 175-mm flasks at a density of 2×10^3 cells/cm^2. Twenty-four hours after seeding, the medium was changed to differentiation medium (L-DMEM, 10% FBS, 5% porcine serum, 3 μmol/L 5-azacytidine (MP Biomedicals), and 100 U/ml penicillin and 100μg/ml streptomycin). After incubating for another 24 hrs, the cells were washed twice with Tyrode's balanced salt solution and the medium was changed to complete medium (L-DMEM, 10% FBS, 5% porcine serum, and 100 U/ml penicillin and 100μg/ml streptomycin). The medium was changed twice a week. Differentiation of BMMCs was verified by sarcomeric α-actinin staining (Sigma). After completing the protocol, aliquots of the cells were prepared for reseeding and immunohistochemistry study. Decellularized scaffolds were sterilized by 70% ethanol for 4 hours and washed by PBS 4 times. After sterilization, decellularized patches were put into T75 tissue culture flask and reseeded with un-selected cells, a mixture of non-differentiated and differentiated BMMCs (10^7 cells/ml) in 50 ml complete medium for 4 hrs under gentle agitation, and then cultured in a 45° inclined rotating bioreactor at a rotation speed of 1Hz. The medium was changed twice every week.

2.4 Histological, SEM, Immunohistochemical Characterizations

Four tissue constructs were prepared for each time point group and subjected to assessments of histology, SEM, and immunohistochemical staining. Filmtracer™ LIVE/DEAD® Biofilm Viability Kit (Invitrogen) solution was prepared by adding 20 μl of the supplied 2 mM EthD-1 stock solution (Component B) to 10 ml of sterile, tissue culture grade D-PBS, vortexing to ensure thorough mixing. The reagents were combined by transferring 5 μl of the supplied 4 mM calcein AM stock solution (Component A) to the 10 ml EthD-1 solution. The reseeded patch was incubated for 30 – 45 minutes at room temperature. Specimens used for light microscopy were fixed in 2% paraformaldehyde solution for 2 hours, embedded in paraffin and stained with hematoxylin and eosin (H&E) and Masson's trichrome. Scanning Electron Microscope (SEM) was also used to verify the existence of vasculature structure in the decellularized scaffolds. After dehydrated in a graded ethanol series, the samples were processed with critical point drying (Polaron E 3000 CPD). The samples were then sputter coated with gold-palladium and observed with SEM (JEOL JSM-6500 FE-SEM).

For immunofluorescent staining, after rehydration and antigen retrieval with 0.05% Trypsin for 10 minutes at 37°C, sections were washed and incubated at 4 °C for overnight with sarcomeric α-actinin (sigma), myosin heavy chain (GenWay), cardiac troponin T, von Willebrand factor (vWF), and Collagen IV (abcam) primary antibodies. After the primary antibody, Cy3 AffiniPure Goat Anti-Mouse IgG (H+L), Cy5 AffiniPure Donkey Anti-Mouse IgM, Alexa Fluor secondary antibodies (JacksonImmuno Research), Goat Anti-Mouse IgG, and Goat Anti-Rabbit IgG secondary antibodies (abcam) were incubated at 37°C for 30 minutes to obtain fluorescent colors. The sections were then stained with Hoechst (Invitrogen) for cell nuclei. Immunohistological slides were observed with an inverted laser scanning confocal microscope (Zeiss LSM 510).

2.5 Biaxial and Uniaxial Mechanical Testing

Tissue biaxial mechanical properties were characterized with a biaxial mechanical testing system.[36] Briefly, a square specimen was trimmed from the native myocardium/engineered patch. Biaxial loading was then applied along muscle/scaffold fiber preferred direction (PD) and cross preferred direction (XD) of the specimen. After 10-cycle preconditioning, the specimen was subjected to biaxial test utilizing an equibiaxial protocol of T_{PD}:T_{XD} = 30:30 N/m, where T_{PD} and T_{XD} were the applied tensions along PD and XD, respectively. Due to possible tissue tear at the hook sites at higher tension level, specimens were loaded up to a maximum tension of 30 N/m. Tissue extensibility was characterized by maximum stretch along PD (λ_{PD}) and maximum stretch along XD (λ_{XD}) at equibiaxial tension of 30 N/m.

A uniaxial machine (Mach-1, Biosyntech, MN) was used to determine tissue mechanical properties. After biaxial testing, tissue strips were cut along PD and were mounted with two stainless steel grips cushioned with emery paper. The tissue was preconditioned for 10 cycles at a ramp speed of 0.1 mm/s. All of the samples were then elongated to failure at the same ramp speed. Stress-strain data in the linear region were fit with linear regression. The tissue extensibility was defined as the intersecting point made by the extrapolation of the linear region with the strain axis, and tensile modulus was determined by finding the tangent of the linear fit. Moreover, failure strength and failure strain were determined from stress-strain data.

Four samples were subjected to mechanical testing for each of the native control, decellularization, 1-week, and 2-week groups. All samples were tested in a PBS bath at 37 °C.

2.6 Statistical Analysis

The experimental data were presented as mean ± standard deviation. One Way Analysis of Variances (ANOVA) was used for statistical analysis, with Holm-Sidak test being used for post hoc pair wise comparisons and comparisons versus the control group (SigmaStat 3.0, SPSS Inc., Chicago, IL). The differences were considered statistically significant when p is less than 0.05.

3. RESULTS

3.1 Acellular Myocardial Scaffold

We found that after 2.5-week decellularization treatment, myocardium showed morphology of white color collagen scaffold, implying decellularization being achieved (Fig. 1-b). Both H&E and Mason's trichrome staining further demonstrated a complete decellularization by the complete lack of cardiomyocytes in the ECM scaffold (Fig. 2-b, c). The longitudinal and transversal views of the acellular scaffold showed that 3D lacunae, previously housing cardiomyocytes, were preserved (Fig. 2-c). The transversal section of acellular myocardial scaffold had an average pore size of 19.5 ± 17.9 μm, which matched transversal dimension of cardiomyocytes. Edge-to-edge views of transversal sections of acellular scaffolds showed that large pores were distributed evenly across the ~2 mm thickness (Fig. 5-a). DAPI staining of the acellular scaffold further verified that no nuclear chromatin fragments remained and a thorough decellularization was achieved (Fig. 3-d). Additionally, part of the vasculature channels was likely preserved. The channel-like structures in histology showed diameters approximately ranging from 100 μm to 400 μm, a size close to small vasculature (Fig. 2-b, c, d: arrows). The preservation of the vascular templates after decellularization was further validated by morphology revealed by SEM (Fig. 3-a), and collagen type IV staining around the channel-like structure (Fig. 3-c, d).

3.2 Recellularization and Phenotype Characterizations

One week after primary culture, BMMCs developed long spindle-shaped cell morphology (Fig. 4-a). BMMC surface antigen profile was positive for CD44 (Fig. 4-b). After 5-azacytidine treatment, sarcomeric α-actinin staining showed positive results (Fig. 4-c). The cardiomyocyte differentiation rate was estimated to be ~24% according to ratio of cells stained positive for sarcomeric α-actinin (Fig. 4-c). A thorough recellularization was verified by Mason's trichrome staining in both the 2-week (Fig. 5-b) and 4-week constructs (Fig. 5-c). In the 2-week construct, cells were found to infiltrate and distribute within the myocardial scaffold. We divided the edge-to-edge section evenly into three regions (2 edge regions and 1 middle region) and measured cell density in each region. Cell densities of the 3 regions in the 2-week constructs were $(2.00 \pm 0.02) \times 10^3/mm^2$, $(1.24 \pm 0.20) \times 10^3/mm^2$, and $(1.69 \pm 0.16) \times 10^3/mm^2$, respectively. Cell densities of the 3 regions in the 4-week constructs were $(2.50 \pm 0.28) \times 10^3/mm^2$, $(1.85 \pm 0.43) \times 10^3/mm^2$, and $(3.11 \pm 0.13) \times 10^3/mm^2$, respectively. In both the 2- and 4-week construct, cell density was evenly distributed found much higher than that of the 2-week construct.

Cell viability was verified by live/dead cell staining (Fig. 6-b,c). Side view of the cross-sectional cut of the construct showed that most cells were alive (Fig. 6-c). However, a ~27% dead cell ratio inside the construct was higher than that on the surface, which had a dead cell ratio less than 5% (Fig. 6-b,c). Immunohistological staining studies showed that the reseeded cells exhibited cardiomyocyte-like phenotype and expressed sarcomeric α-actinin, myosin heavy chain and cardiac troponin T (Fig. 7-b, d, f). Moreover, vWF factor were found around vessel-like structures, implying possible endothelialization inside vasculature channels (Fig. 7-g).

3.3 Mechanical Properties

We found that both native myocardium and acellular scaffold showed anisotropic nonlinear behavior (Fig. 8-a, b), in which muscle fiber-preferred direction was stiffer than cross fiber-preferred direction (Fig. 8-a). After removal of muscle cells, both PD and XD directions showed stiffer stress-strain curves (Fig. 8-b). We later found that tissue remodeling caused a recovery of the biaxial mechanical properties after 1-week and 2-week recellularization (Fig. 8-c, d). The 1-week and 2-week tissue constructs kept nonlinear anisotropic behavior and tissue extensibility more close to native myocardium along both PD and XD directions (Table 1; Fig. 8-c, d). The stiffer mechanical properties of the decellularized myocardial scaffolds were also verified by uniaxial testing results (Fig. 9-a, b). Similar to biaxial characterization, after 1-week and 2-week cultures, constructs showed a recovering tendency (Fig. 9). Tensile modulus, tissue extensibility, and failure stress are listed in Table 1 for native myocardium, decellularized scaffold, 1-week, and 2-week tissue constructs.

4. DISCUSSION

Fabrication of 3D scaffolds that are thoroughly reseeded with cells remains a challenge for making a viable thick cardiac patch.[21,22,24,25,37] Although engineered patches have been found to partially restore cardiac function,[37] engineered myocardial tissues generate relatively low contractile force that is not sufficent to contribute to normal heart function.[13,38] Other challenges include diffusion limitation, lack of seeded cell differentiation, inferior electrophysiological function,[37,39] and unmatched mechanical properties.[37] To overcome the above obstacles, the ideal scaffold should closely resemble the structure of native myocardial extracellular matrix (ECM) that provides ultrastructural, mechanical, and componential cues for cardiomyocyte functions.[12-15]

The histological study showed that the collagen network previously wrapping around muscle cells maintained the pore structure (Fig. 2). Our edge-to-edge view of the cross-section demonstrated that the open porous structure could maintain across a large area without collapse (Fig. 5-a). It is evident that the cardiac collagen network appears to be a strong 3D structure, probably required for adequate cardiac functioning (extension of the cardiac "skeleton"). Another interesting finding was that vasculature templates (vessel-like structure) were possibly preserved after decellularization, according to our histological observations (Fig. 2), SEM (Fig. 3-a), and collagen type IV staining (Fig. 3-b, c).

In this exploratory study, we chose BMMCs as our reseeding cell source. The isolated BMMCs had strong self-renewal ability and 70% of the cells were mesenchymal stem cells and positive for CD44, a cell-surface glycoprotein of mesenchymal stem cells (MSCs).[40] BMMCs were previously reported to have the ability to differentiate into cardiomyocyte phenotype under specific culture conditions as well as in healthy and infarcted myocardium (e.g., injection in animal models).[41-45] BMMCs were found to secrete angiogenic cytokines that promote blood flow recovery in a murine hind limb ischemia model.[46]

5-azacytidine is a member of the cytosine analogue, which had been reported to have the ability to change cell phenotypes by activating novel gene expressions both in vitro and in vivo.[47] It was reported that after 5-azacytidine treatment, about 30% cardiomyocyte differentiation took place in culture.[48,49] We showed that, after BMMCs were treated with 5-azacytidine for 24 hours, the treated cells exhibited myocyte-like phenotype and were positive for sarcomeric α-actinin (Fig. 4-c). A higher magnification of the differentiated cells showed visible sarcomere alignment (Fig. 4-d), further verifing the myocyte-like morphology. The successful recellularization of the 5-azacytidine treated BMMCs verified our hypothesis that the acellular porous myocardial scaffold provided an optimal recellularization microenvironment.

Reseeded cells were found to infiltrated and proliferate well in the tissue construct (Fig. 5). The cell density in 4-week construct was higher than 2-week construct. From the live/dead staining results, it was shown that the proliferation rate of the reseeded cells remained high in 4-week *in vitro* culture. The cells were found distributed evenly across the 2 mm thick patch, indirectly proving the interconnectivity of 3D myocyte lacunae after decellularization. As we know, thorough and uniform recellularization at high cell density was a prerequisite for the later success of functional cardiac tissue constructs. Note that our reseeding data showed thorough reseeding, but the level of uniformity and cell density may be insufficient and require further investigation to improve our reseeding technique.

Phenotypic characterizations showed that cells in the engineered patch were positive for sarcomeric α-actinin, MHC, and cardiac troponoin T (Fig. 7-b, d, f), which suggested a differentiation into a cardiomyocyte-like phenotype. In the engineered patch, vWF expression (endothelial marker) was verified at locations with vessel-like histological structure (Fig.7-c). Moreover, Hoechst staining showed the cell nuclei aligned along the inner surface of the vessel-like structure. The above observations revealed that possible endothelialization took place around the vasculature templates, implying potential for angiogenesis in the engineered patch. The detailed mechanism is unclear. We speculate that undifferentiated mesenchymal stem cells might be the underlying mechanism of endothelialization along the vasculature channels in the engineered patches.

Our biaxial and uniaxial mechanical testing results also provided potential mechanistic insight into how reseeded cells remodeled the engineered scaffolds. After the removal of cardiomyocytes, mechanical properties of the remaining ECM, consisting of mainly collagen, were measured. It was thus understandable that both PD and XD directions showed stiffer curves. The preservation of anisotropic properties (Fig. 8-b) was due to the orientation of ECM lacunae, which aligned most collagen fibers along muscle fiber-preferred direction (Fig. 2-c) (note that muscle cells were removed). The increase of cellular content explained the recovery of the biaxial mechanical properties after reseeding for 1 week and 2 weeks (Fig. 8-c, d). The uniaxial testing results also demonstrated obvious tissue remodeling in the 2-week constructs, which exhibited greater tissue extensibility and lower failure stress (Fig. 9-b; Table 1). Overall, the mechanical properties of the reseeded scaffolds showed a recovering trend along with the culture time, as expected from the increased cellular content (Fig. 5). It had been reported that the “passive stiffness” of the myocardium is a major determinant of overall cardiac function.[50,51] Thus, it was of importance to have an engineered cardiac patch that matched the mechanical properties of native myocardium. We have found that the mechanical properties of the two-week scaffold were close to the native myocardium; however, further studies are needed in order to obtain higher cell density, cell interconnection, and electrophysiological properties.

5. CONCLUSIONS

In this study, we successfully developed acellular myocardial scaffold with well-preserved ECM structure. We observed recellularization with good cell viability, ingrowth, proliferation, and differentiation. Both uniaxial and biaxial mechanical studies demonstrated the positive tissue remodeling in the engineered patch. Future study will focuse on improving reseeding density, cell alignment and interconnection, and facilitating mesenchymal stem cell differentiation via *in vitro* conditioning using a bioreactor that provides coordinated mechanical and electrical stimulations. The clinical product that we envision will benefit from the natural architecture of myocardial ECM, which has potential to promote stem cell differentiation, cardiac regeneration, and angiogenesis.

6. LIMITATIONS

It was found that cell alignment and interconnection were not ideal in the constructs, most likely due to sub-physiological cell density and collapse of scaffold pores in the tissue culture procedure. In order to obtain high density reseeding, needle injection and flow perfusion reseeding approaches will be evaluated in the future. Collapse of the pores might take place in the reseeding and tissue culture period, consequently causing the nonuniformity in the recellularization and poor cell interconnection. A specimen receptacle will be designed to retain scaffold macrogeometry, consequently preventing scaffold contraction and porous structure collapse. Note that the current study is mainly focused on scaffold development and assessments. In the future study, well-characterized bone marrow MSCs will be obtained and electrophysiological parameters of engineered patch will be determined using microelectrode array technique.

Acknowledgments

This work was supported by NIH National Heart, Lung, and Blood Institute grant HL097321. The authors also would like acknowledge the support from the MAFES Strategic Research Initiative Funding (CRESS MIS-741110) and the Health Resources and Services Administration (HRSA) (DHHS R1CRH10429-01-00). The authors thank Dr. Michael S. Sacks (University of Pittsburgh) for supporting on biaxial device building, and thank Dr. Giselle Thibaudeau, William Monroe, Amanda Lawrence (MSU EM center) and Scott Metzler for help on histology, imaging, and discussion. Support from Sansing Meat Service (Maben, MS) is also greatly appreciated.

References

1. American Heart Association. Heart and stroke statistical update. American Heart Association; Dallas [TX]: 2002.
2. Cleutjens JP, Blankesteijn WM, Daemen MJ, Smits JF. The infarcted myocardium: simply dead tissue, or a lively target for therapeutic interventions. Cardiovasc Res. 1999; 44(2):232–41. [PubMed: 10690298]
3. De Celle T, Cleutjens JP, Blankesteijn WM, Debets JJ, Smits JF, Janssen BJ. Long-term structural and functional consequences of cardiac ischaemia-reperfusion injury in vivo in mice. Exp Physiol. 2004; 89(5):605–15. [PubMed: 15258119]
4. Leor J, Aboulafia-Etzion S, Dar A, Shapiro L, Barbash IM, Battler A, Granot Y, Cohen S. Bioengineered cardiac grafts: A new approach to repair the infarcted myocardium? Circulation. 2000; 102(19 Suppl 3):III56–61. [PubMed: 11082363]
5. Swynghedauw B. Molecular mechanisms of myocardial remodeling. Physiol Rev. 1999; 79(1):215–62. [PubMed: 9922372]
6. Topol EJ. Current status and future prospects for acute myocardial infarction therapy. Circulation. 2003; 108(16 Suppl 1):III6–13. [PubMed: 14605014]
7. Sharma R, Raghubir R. Stem cell therapy: a hope for dying hearts. Stem Cells Dev. 2007; 16(4): 517–36. [PubMed: 17784827]
8. Grauss RW, Winter EM, van Tuyn J, Pijnappels DA, Steijn RV, Hogers B, van der Geest RJ, de Vries AA, Steendijk P, van der Laarse A. Mesenchymal stem cells from ischemic heart disease patients improve left ventricular function after acute myocardial infarction. Am J Physiol Heart Circ Physiol. 2007; 293(4):H2438–47. others. [PubMed: 17644573]
9. Strauer BE, Kornowski R. Stem cell therapy in perspective. Circulation. 2003; 107(7):929–34. [PubMed: 12600901]
10. Ozawa T, Mickle DA, Weisel RD, Koyama N, Wong H, Ozawa S, Li RK. Histologic changes of nonbiodegradable and biodegradable biomaterials used to repair right ventricular heart defects in rats. J Thorac Cardiovasc Surg. 2002; 124(6):1157–64. [PubMed: 12447182]
11. Ozawa T, Mickle DA, Weisel RD, Koyama N, Ozawa S, Li RK. Optimal biomaterial for creation of autologous cardiac grafts. Circulation. 2002; 106(12 Suppl 1):I176–82. [PubMed: 12354729]
12. Langer R, Vacanti JP. Tissue Engineering. Science. 1993; 260:920–926. [PubMed: 8493529]

13. Zimmermann WH, Melnychenko I, Eschenhagen T. Engineered heart tissue for regeneration of diseased hearts. Biomaterials. 2004; 25(9):1639–47. [PubMed: 14697865]
14. Thompson RB, Emani SM, Davis BH, van den Bos EJ, Morimoto Y, Craig D, Glower D, Taylor DA. Comparison of intracardiac cell transplantation: autologous skeletal myoblasts versus bone marrow cells. Circulation. 2003; 108(Suppl 1):II264–71. [PubMed: 12970244]
15. Bursac N, Papadaki M, Cohen RJ, Schoen FJ, Eisenberg SR, Carrier R, Vunjak-Novakovic G, Freed LE. Cardiac muscle tissue engineering: toward an in vitro model for electrophysiological studies. Am J Physiol. 1999; 277(2 Pt 2):H433–44. [PubMed: 10444466]
16. Kellar RS, Shepherd BR, Larson DF, Naughton GK, Williams SK. Cardiac patch constructed from human fibroblasts attenuates reduction in cardiac function after acute infarct. Tissue Eng. 2005; 11(11-12):1678–87. [PubMed: 16411813]
17. Barandon L, Couffinhal T, Dufourcq P, Alzieu P, Daret D, Deville C, Duplaa C. Repair of myocardial infarction by epicardial deposition of bone-marrow-cell-coated muscle patch in a murine model. Ann Thorac Surg. 2004; 78(4):1409–17. [PubMed: 15464506]
18. Aboulafia-Etzion S, Leor J, Barbash IM, Battler A. Fixing a failing heart: molecular and cellular approaches. Harefuah. 1999; 136(4):284–8. [PubMed: 10914220]
19. Wei HJ, Chen CH, Lee WU, Chiu I, Hwang SW, Lin WW, Huang CC, Yeh YC, Chang Y, Sung HW. Bioengineered cardiac patch constructed from multilayered mesenchymal stem cells for myocardial repair. Biomaterials. 2008 Epub.
20. Tan MY, Zhi W, Wei RQ, Huang YC, Zhou KP, Tan B, Deng L, Luo JC, Li XQ, Xie HQ. Repair of infarcted myocardium using mesenchymal stem cell seeded small intestinal submucosa in rabbits. Biomaterials. 2009; 30(19):3234–40. others. [PubMed: 19261327]
21. Carrier RL, Papadaki M, Rupnick M, Schoen FJ, Bursac N, Langer R, Freed LE, Vunjak-Novakovic G. Cardiac tissue engineering: cell seeding, cultivation parameters, and tissue construct characterization. Biotechnol Bioeng. 1999; 64(5):580–9. [PubMed: 10404238]
22. Birla RK, Borschel GH, Dennis RG, Brown DL. Myocardial engineering in vivo: formation and characterization of contractile, vascularized three-dimensional cardiac tissue. Tissue Eng. 2005; 11(5-6):803–13. [PubMed: 15998220]
23. Birla RK, Borschel GH, Dennis RG. In vivo conditioning of tissue-engineered heart muscle improves contractile performance. Artif Organs. 2005; 29(11):866–75. [PubMed: 16266299]
24. Borschel GH, Dow DE, Dennis RG, Brown DL. Tissue-engineered axially vascularized contractile skeletal muscle. Plast Reconstr Surg. 2006; 117(7):2235–42. [PubMed: 16772923]
25. Vouyouka AG, Powell RJ, Ricotta J, Chen H, Dudrick DJ, Sawmiller CJ, Dudrick SJ, Sumpio BE. Ambient pulsatile pressure modulates endothelial cell proliferation. J Mol Cell Cardiol. 1998; 30(3):609–15. [PubMed: 9515036]
26. Kajstura J, Rota M, Whang B, Cascapera S, Hosoda T, Bearzi C, Nurzynska D, Kasahara H, Zias E, Bonafe M. Bone marrow cells differentiate in cardiac cell lineages after infarction independently of cell fusion. Circ Res. 2005; 96(1):127–37. others. [PubMed: 15569828]
27. Streeter DD Jr. Hanna WT. Engineering mechanics for successive states in canine left ventricular myocardium. II. Fiber angle and sarcomere length. Circ Res. 1973; 33(6):656–64. [PubMed: 4762007]
28. Streeter DD Jr. Spotnitz HM, Patel DP, Ross J Jr. Sonnenblick EH. Fiber orientation in the canine left ventricle during diastole and systole. Circ Res. 1969; 24(3):339–47. [PubMed: 5766515]
29. Macchiarelli G, Ohtani O. Endomysium in left ventricle. Heart. 2001; 86(4):416. [PubMed: 11559682]
30. Gilbert TW, Sellaro TL, Badylak SF. Decellularization of tissues and organs. Biomaterials. 2006; 27(19):3675–83. [PubMed: 16519932]
31. Liao J, Joyce EM, Sacks MS. Effects of decellularization on mechanical and structural properties of the porcine aortic valve leaflets. Biomaterials. 2008; 29(8):1065–74. [PubMed: 18096223]
32. Borschel GH, Huang YC, Calve S, Arruda EM, Lynch JB, Dow DE, Kuzon WM, Dennis RG, Brown DL. Tissue engineering of recellularized small-diameter vascular grafts. Tissue Eng. 2005; 11(5-6):778–86. [PubMed: 15998218]

33. Borschel GH, Dennis RG, Kuzon WM Jr. Contractile skeletal muscle tissue-engineered on an acellular scaffold. Plast Reconstr Surg. 2004; 113(2):595–602. discussion 603-4. [PubMed: 14758222]
34. Badylak SF, Tullius R, Kokini K, Shelbourne KD, Klootwyk T, Voytik SL, Kraine MR, Simmons C. The use of xenogeneic small intestinal submucosa as a biomaterial for Achilles tendon repair in a dog model. J Biomed Mater Res. 1995; 29(8):977–85. [PubMed: 7593041]
35. Ott HC, Matthiesen TS, Goh SK, Black LD, Kren SM, Netoff TI, Taylor DA. Perfusion-decellularized matrix: using nature's platform to engineer a bioartificial heart. Nat Med. 2008; 14(2):213–21. [PubMed: 18193059]
36. Grashow JS, Yoganathan AP, Sacks MS. Biaixal stress-stretch behavior of the mitral valve anterior leaflet at physiologic strain rates. Ann Biomed Eng. 2006; 34(2):315–25. [PubMed: 16450193]
37. Robinson KA, Li J, Mathison M, Redkar A, Cui J, Chronos NA, Matheny RG, Badylak SF. Extracellular matrix scaffold for cardiac repair. Circulation. 2005; 112(9 Suppl):I135–43. [PubMed: 16159805]
38. Zimmermann WH, Eschenhagen T. Cardiac tissue engineering for replacement therapy. Heart Fail Rev. 2003; 8(3):259–69. [PubMed: 12878835]
39. Bursac N, Loo Y, Leong K, Tung L. Novel anisotropic engineered cardiac tissues: studies of electrical propagation. Biochem Biophys Res Commun. 2007; 361(4):847–53. [PubMed: 17689494]
40. Vogel W, Grunebach F, Messam CA, Kanz L, Brugger W, Buhring HJ. Heterogeneity among human bone marrow-derived mesenchymal stem cells and neural progenitor cells. Haematologica. 2003; 88(2):126–33. [PubMed: 12604402]
41. Wollert KC, Drexler H. Mesenchymal stem cells for myocardial infarction: promises and pitfalls. Circulation. 2005; 112(2):151–3. [PubMed: 16009806]
42. Makino S, Fukuda K, Miyoshi S, Konishi F, Kodama H, Pan J, Sano M, Takahashi T, Hori S, Abe H. Cardiomyocytes can be generated from marrow stromal cells in vitro. J Clin Invest. 1999; 103(5):697–705. others. [PubMed: 10074487]
43. Toma C, Pittenger MF, Cahill KS, Byrne BJ, Kessler PD. Human mesenchymal stem cells differentiate to a cardiomyocyte phenotype in the adult murine heart. Circulation. 2002; 105(1): 93–8. [PubMed: 11772882]
44. Mangi AA, Noiseux N, Kong D, He H, Rezvani M, Ingwall JS, Dzau VJ. Mesenchymal stem cells modified with Akt prevent remodeling and restore performance of infarcted hearts. Nat Med. 2003; 9(9):1195–201. [PubMed: 12910262]
45. Shake JG, Gruber PJ, Baumgartner WA, Senechal G, Meyers J, Redmond JM, Pittenger MF, Martin BJ. Mesenchymal stem cell implantation in a swine myocardial infarct model: engraftment and functional effects. Ann Thorac Surg. 2002; 73(6):1919–25. discussion 1926. [PubMed: 12078791]
46. Kinnaird T, Stabile E, Burnett MS, Shou M, Lee CW, Barr S, Fuchs S, Epstein SE. Local delivery of marrow-derived stromal cells augments collateral perfusion through paracrine mechanisms. Circulation. 2004; 109(12):1543–9. [PubMed: 15023891]
47. Chiu CP, Blau HM. 5-Azacytidine permits gene activation in a previously noninducible cell type. Cell. 1985; 40(2):417–24. [PubMed: 2578323]
48. Tomita Y, Makino S, Hakuno D, Hattan N, Kimura K, Miyoshi S, Murata M, Ieda M, Fukuda K. Application of mesenchymal stem cell-derived cardiomyocytes as bio-pacemakers: current status and problems to be solved. Med Biol Eng Comput. 2007; 45(2):209–20. [PubMed: 17262204]
49. Fukuda K. Regeneration of cardiomyocytes from bone marrow: Use of mesenchymal stem cell for cardiovascular tissue engineering. Cytotechnology. 2003; 41(2-3):165–75. [PubMed: 19002953]
50. Holmes JW, Borg TK, Covell JW. Structure and mechanics of healing myocardial infarcts. Annu Rev Biomed Eng. 2005; 7:223–53. [PubMed: 16004571]
51. Humphery, JD. Cardiovascular Solid Mechanics. Springer Verlag; 2002.

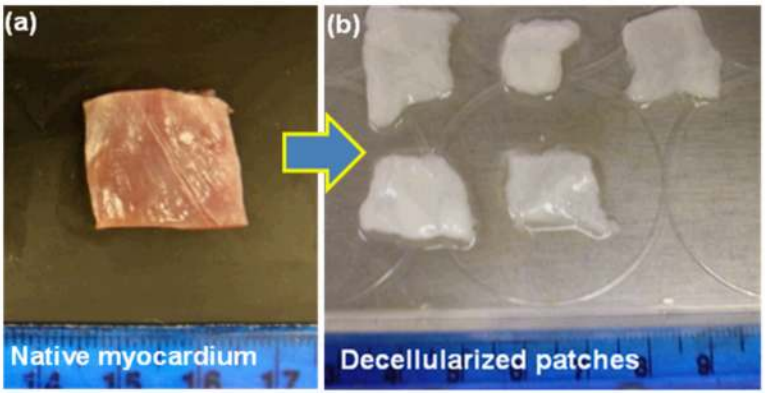

Figure 1.
Morphology of (a) native myocardium and (b) decellularized myocardial scaffold. Thorough decellularization was achieved after 2.5 weeks treatment.

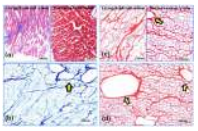

Figure 2.
Mason's trichrome staining for (a) native myocardium and (b) decellularized myocardial scaffold (blue: collagen, red/pink: cardiomyocytes). (c) H&E staining of the longitudinal and transversal views of the acellular scaffold showed that 3D lacunae housing cardiomyocytes were preserved (red: collagen). (d) Vasculature templates in the decellularized myocardial scaffold (H&E staining). Arrows indicate vasculature channels.

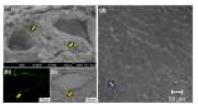

Figure 3.

Preservation of vasculature structure was verified by (a) SEM and (b) type IV collagen staining (green color) on the circular structure; (c) transmission light image of the same region shown in (b). Arrows in (a), (b), and (c) indicate the existence of vasculature templates. (d) A combined image of the DAPI staining (blue color) and the transmission light image on the section of the decellularized scaffolds. Lack of DAPI staining verified that no nuclear chromatin fragments remained in the scaffolds. Arrow in (d) showed a minute spot of DAPI stain (blue color).

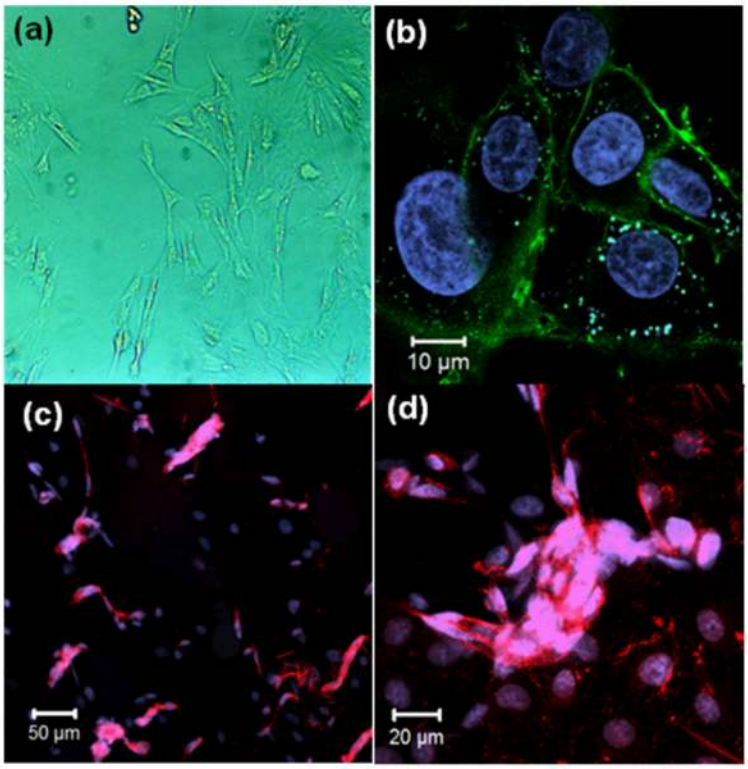

Figure 4.
(a) BMMCs after one week primary culture. (b) Positive staining for stem cell marker CD44 (green color). (c) Cardiomyocyte differentiation after treatment with 5-azacytinine; (d) a higher magnification of the differentiated cells with visible sarcomere alignment. Red staining: sarcomeric α-actinin.

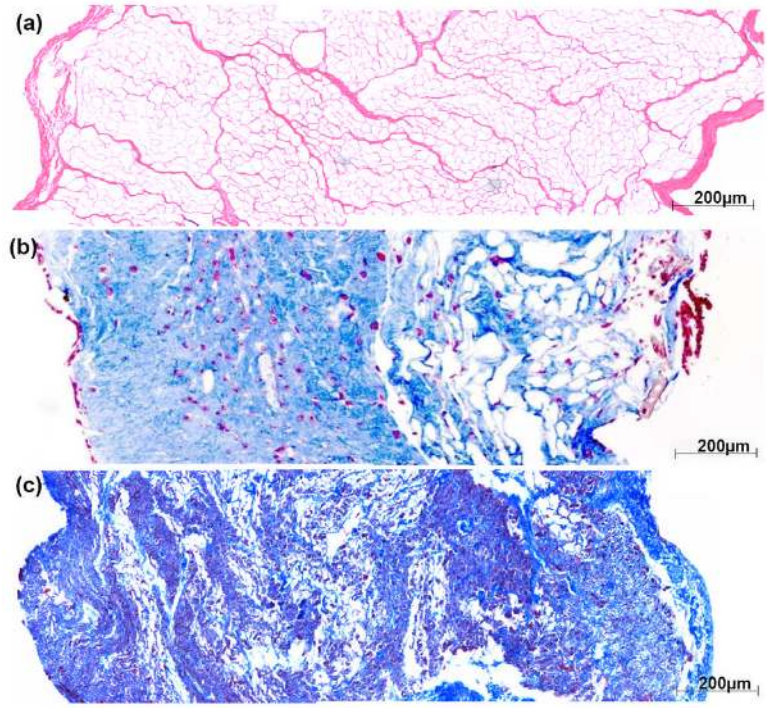

Figure 5.
(a) Large pores distributing evenly across the 2 mm thick acellular scaffold (H&E). (b) Edge-to-edge view of thorough recellularization at 2 weeks, in which cells were found to infiltrate and distribute within the myocardial scaffold. (c) Tissue remodeling was observed in the 4-week recellularization tissue construct; even cell distribution was still observed and cell density was found higher than that of the 2-week construct.

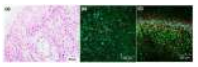

Figure 6.
(a) Thorough and relatively dense reseeding was observed in tissue construct after 4-week culture (H&E staining). Live/dead cell staining on 4-week tissue construct: (b) surface of tissue construct and (c) side view of cross-sectional cut. Green: living cells; red: dead cells.

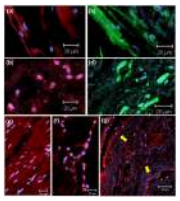

Figure 7.
Sarcomeric α-actinin staining (red) in the native myocardium (a) and the reseeded patch (b); myosin heavy chain staining (green) in the native myocardium (c) and the reseeded patch (d); cardiac troponin T staining (red) in the native myocardium (e) and the reseeded patch (f). vWF factor (red) was shown in the reseeded patch (g). Cell nucleus: blue.

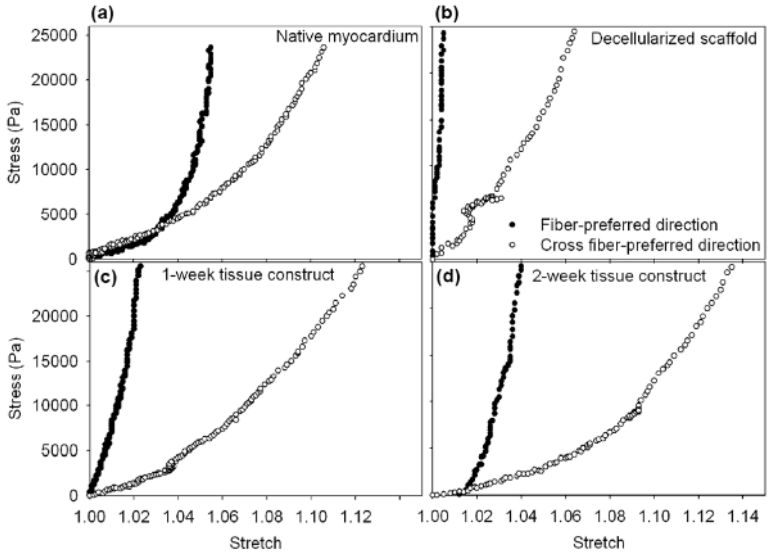

Figure 8.

Biaxial mechanical properties. (a) Native myocardium showed anisotropic nonlinear behavior, in which muscle fiber-preferred direction (PD) is stiffer than cross fiber-preferred direction (XD). (b) PD and XD directions showed stiffer stress-strain curves in decellularized myocardial scaffold (c) 1 week reseeded cardiac patch (d) 2 weeks reseeded cardiac patch. Tissue remodeling caused a recovery of the biaxial mechanical properties after 1-week and 2-week recellularization. The 1-week and 2-week tissue constructs kept nonlinear anisotropic behavior and tissue extensibility more close to native myocardium along both PD and XD directions.

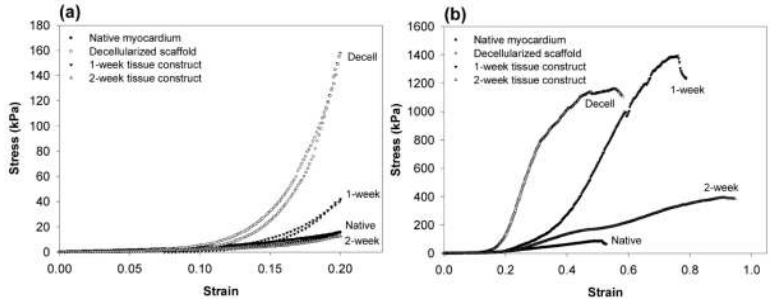

Figure 9.

Both (a) uniaxial mechanical properties and (b) tissue failure properties show a recovering tendency after 1-week and 2-week cultures. Note that both loading and unloading stress-strain curves were shown in (a).

Table 1

Biaxial and uniaxial mechanical properties of native myocardium, decellularized scaffold, and patch constructs.

	Biaxial Mechanical Properties		**Uniaxial Mechanical Properties**		
	Maximum stretch (PD)	Maximum stretch (XD)	Tensile modulus (kPa)	Extensibility (strain)	Failure stress (kPa)
Native myocardium	1.083 ± 0.029	1.145 ± 0.048	223.3 ± 49.2	0.199 ± 0.050	67.5 ± 25.1
Decellularized scaffold	1.004 ± 0.006*	1.150 ± 0.008	5218.7± 1723.5*	0.169 ± 0.003	903.0 ± 363.5
1-week construct	1.060 ± 0.006	1.150 ± 0.053	3593.2± 838.9*	0.198 ± 0.074	914.0 ± 673.2
2-week construct	1.040 ± 0.037	1.210 ± 0.009	760.6 ± 69.7	0.216 ± 0.012	482.5 ± 85.6

*denotes significant difference when compared with native myocardium ($p < 0.05$).